Available online at www.sciencedirect.com
ScienceDirect
Journal of the European Ceramic Society 27 (2007) 807–812
www.elsevier.com/locate/jeurceramsoc

Effect of forming pressure on densification behavior of nanocrystalline ITO powder

Bong-Chull Kim, Joon-Hyung Lee, Jeong-Joo Kim *

Department of Inorganic Materials Engineering, Kyungpook National University, Daegu 702-701, Republic of Korea

Available online 2 June 2006

Abstract

Since ultrafine nano-particles easily produce agglomerates, they result in an inhomogeneous particle packing structure within a green body. Nanocrystalline indium tin oxide (ITO) powder was prepared, and the compaction behavior of the powder was investigated by using an Hg porosimetry and a scanning electron microscope (SEM) as a function of the applied cold isostatic pressing (CIP) pressure. In addition, the sintering behavior of the compact was monitored with a thermo-mechanical analyzer (TMA), and the relationship between the inhomogeneity in the green body and the sintering behavior was examined. An increase in the forming pressure enhanced the homogeneity of the powder compact by crushing the larger agglomerates. The first generation agglomerate compact showed a two-step densification process in the shrinkage rate curve of TMA. The two-step densification behavior is explained by the elimination of two kinds of pores, which are small inter-crystallite pores and large inter-first generation agglomerate pores.

Keywords: Pressing; Sintering; Porosity; Nanocrystalline powder

1. Introduction

Decades of research on conventional ceramic processing have shown that the uniformity and homogeneity of a green body had an enormous impact on how well the green body will densify during sintering. Due to the ultrafine particle size of the nanocrystalline powders, they are quite susceptible to the formation of interparticle London–van der Waals bonds either in the wet or in the dry state.[1] The van der Waals attraction can cause the powder particles to bond together into agglomerates during handling, drying, or storage.[2] Therefore, the compaction of these fractal-like agglomerates produces an inhomogeneous particle packing structure within a green body, which results in poor green density.[3] Nanocrystalline powders are problematic in this regard.

One substantial problem, which is not correlated with agglomeration, is the large number of particle–particle point contacts per unit volume in a compact composed of nanocrystalline powder, as compared with the one composed of micrometer-sized particles.[2] Each of these point contacts represents a source of frictional resistance between particles. Thus, the total frictional resistance can be much greater for nanocrystalline powders than for larger particles. Consequently, for a given applied stress during compaction, in the case of nanocrystalline powders, less particle–particle sliding and particle rearrangement are anticipated than one might expect for a conventional powder. In the uniaxial pressure the application of higher stress can force nanoparticles to slide against each other thus forming a denser packing arrangement, but large residual stress can be set up in a green body, causing the green body to fracture during subsequent handling or sintering.

For the same level of applied stress, one can thus obtain a much more homogeneous particle packing by cold isostatic pressing (CIP) than by uniaxial pressing. Therefore, larger and more solid specimens are produced by CIP. However, a typical CIP is limited to a pressure amount of ∼550 MPa and cannot reach the GPa pressure, which is favored by many researchers for the fabrication of a compact homogeneous nanocrysatilline powder. Therefore, an inhomogeneous compact is frequently fabricated when nanocrystalline powders are used.[4] However, compaction characteristics of the nanocrystalline powders and their sintering behaviors have not been investigated in detail yet.

* Corresponding author. Tel.: +82 53 950 5635; fax: +82 53 950 5645.
E-mail address: jjkim@knu.ac.kr (J.-J. Kim).

0955-2219/$ – see front matter © 2006 Elsevier Ltd. All rights reserved.
doi:10.1016/j.jeurceramsoc.2006.04.033

Since one of the most widely used nanocrystalline ceramics for the application of transparent conducting oxide is indium tin oxide (ITO), many researchers have focused on the preparation of homogeneous nano-sized powders and their densification behaviors.[5] To produce highly dense ITO targets, which affect the sputtering efficiency and properties of sputtered films, nanocrystalline ITO powders have been cold isostatically pressed and sintered in an oxygen atmosphere.[6,7] In this study, nanocrystalline ITO powder was prepared. The inhomogeneity in the nanocrystalline powder compact was controlled by changing the CIP pressure and its compaction behavior was investigated using an Hg porosimetry and a scanning electron microscope (SEM). In addition, the sintering behavior of the compact was monitored with a thermo-mechanical analyzer (TMA), and the relationship between the inhomogeneity in the green body and the sintering behavior was examined.

2. Experimental

Nanocrystalline $8SnO_2$–$92In_2O_3$ (in at.%) powders were prepared by a coprecipitation method. Indium nitrate ($In(NO_3)_3{\cdot}5.7H_2O$, 99.99%) and tin chloride ($SnCl_4{\cdot}5H_2O$, 99.9%) were used as starting chemicals. A mixed solution of $8SnO_2$–$92In_2O_3$ was prepared. NH_4OH was added to a continuously stirred bath of the mixed solution. The final pH of the solution was adjusted to 9.5. Then, the precipitate was separated by filtering and washed several times with distilled water to remove any residual Cl^- and NO_3^- ions. The $AgNO_3$ solution was used to trace the residual Cl^- ions. The dried precipitate was calcined at 600 °C for 1 h. Powder X-ray diffraction with nickel-filtered Cu Kα radiation (Model; M03XHF, Mac Science, Yokohama, Japan) was used for phase identification and particle size measurement. The morphology and size of the ITO powder were examined by transmission electron microscopy (TEM, Model; H-7100, Hitachi, Tokyo, Japan). The relative surface area of the ITO powder was measured by a BET (Model; Asap 2010, Micromeritics, Norcross, USA) and the particle size was also calculated from the data. The In/Sn atomic ratio and impurities in the starting ITO powder were analyzed by an X-ray fluorescence spectrometer (XRF, Model; PW 2400, Phillips, Eindhoven, The Netherlands). The XRF analysis of the ITO powder revealed a composition of (8.2 ± 0.2)Sn–(91.8 ± 0.2)In. The ITO powder was formed into pellets by a sequential process of uniaxial pressing, followed by cold isostatic pressing. In uniaxial pressing, a weak pressure of 5 MPa was applied to the powder in a steel die 10 mm in diameter. The subsequent CIP of the green compacts was conducted at pressure of 25, 50, 100, and 300 MPa, respectively. The pore size distribution of the powder compacts was measured with Hg porosimetry (Model; Macropores unit 120/Porosimeter 2000, Carlo Erba Instruments, Italy). The densification behavior of the powder compacts, which formed at different pressure was monitored using a thermo-mechanical analyzer (Model; TMA 1700, Rigaku, Tokyo, Japan). The agglomerate morphology of the starting ITO powder and fracture surfaces of the samples were observed using a scanning electron microscope (Model; Hitachi S-4200, Tokyo, Japan).

3. Results and discussion

Fig. 1 shows the X-ray diffraction pattern of the ITO powder calcined at 600 °C for 1 h. Diffraction peaks were observed at positions corresponding to the cubic ITO.[8] The average crystallite radius calculated from the X-ray peak broadening and BET surface area was 15 and 13 nm, respectively.

The TEM and SEM images of the starting ITO powder are presented in Fig. 2. The TEM images show that spherical and longish shaped particles with a radius range between 6 and 17 nm coexisted. The low magnification SEM image in Fig. 2(b) shows the morphology and the size of the agglomerates. Irregular agglomerates in a range of several ten micrometers were observed in the starting powder. Fig. 2(c) is the enlarged photograph of Fig. 2(b). In Fig. 2(b) and (c), multiple generations of agglomerates are portrayed from the viewpoint of fractal geometry, i.e. the first generation is a cluster of crystallites, and the second generation is a cluster of these clusters. Successive generations are clusters of clusters at higher scales. Onoda and Toner[3] has suggested that over the size range which the generations span, this structure that is characterized by multiple generations of agglomerates is fractal.

Fig. 3 shows the cumulative pore size distribution in ITO green bodies prepared under various forming pressure. The cumulative pore size distribution curve of 25 MPa has many bending points, as indicated by arrows in Fig. 3, which implies that many pores with different sizes exist in the green body. From the cumulative pore size distribution curve of 25 MPa, which was compacted at the lowest pressure, it is concluded from the distribution of the agglomerates in the starting powders that the starting powder is composed of multiple generations of agglomerates. At 50 MPa, pores larger than 100 nm were eliminated in the powder compact and only pores between 10 and 100 nm remained, which implies that large agglomerates which produced inter-agglomerate pores larger than 100 nm were completely broken down and then eliminated in the compact. At a pressure of 100 MPa, pores larger than 10 nm were eliminated and pores smaller than 10 nm remained, moreover, no bending point was observed in the curve. When the forming pressure

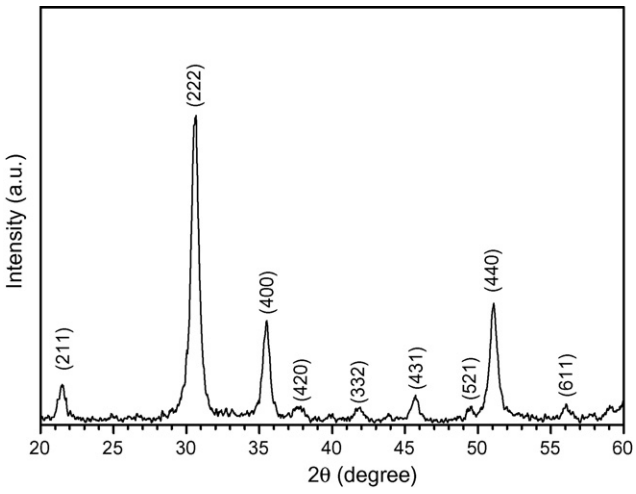

Fig. 1. The X-ray diffraction patterns of the starting ITO powders.

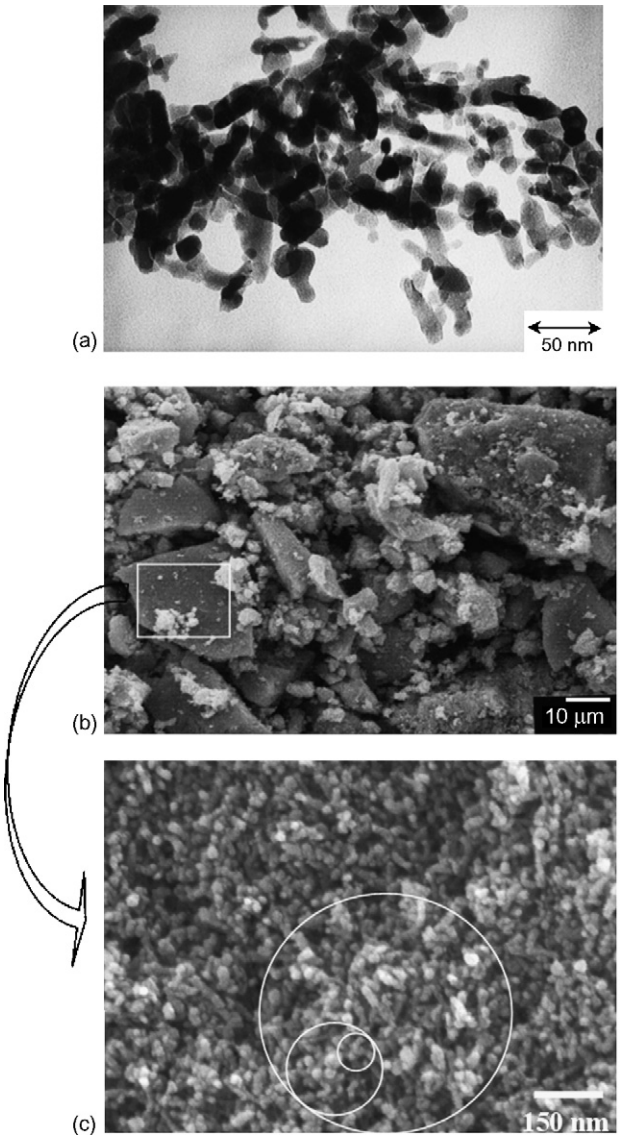

Fig. 2. Crystallite and agglomerate morphology of the ITO starting powder: (a) TEM image, (b) SEM image of low magnification, and (c) SEM image of high magnification.

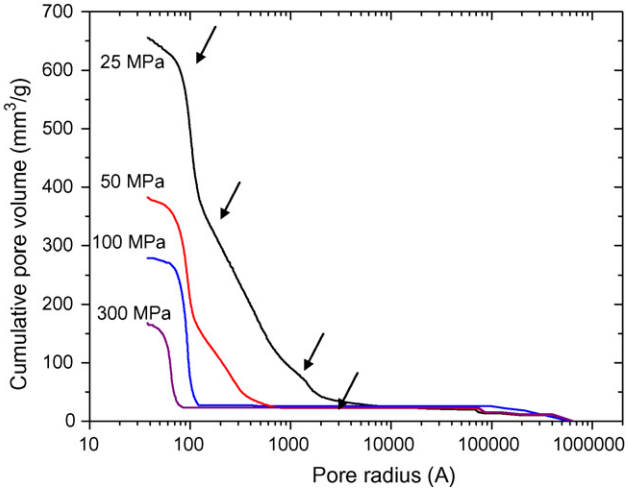

Fig. 3. Cumulative pore size distribution in the ITO green bodies formed at various pressure levels.

increased from 100 to 300 MPa, the average pore radii of the powder compact slightly decreased from 9 to 7 nm, without a change in the curve type. Assuming that the radius of the powder used in this experiment is 15 nm with a spherical shape, and that it is packed in a face-centered cubic (fcc) arrangement, the radius of small spaces, with a coordination number of 4 and large spaces with a coordination number of 6, are 3.4 and 6.2 nm, respectively. Since a general mercury porosimeter cannot analyze exact pores below 5 nm in radius and as the inter-crystallite spaces of the powders used in this experiment roughly agree with the measurable limit, it is difficult to measure the inter-crystallite pore size. Therefore, the cumulative pore volume of all powder compacts, increase sluggishly within a pore radius range of <6 nm (60 Å), which corresponds to that of the inter-crystallite pores in the nanocrystalline ITO powder compact. This implied that pores in the radius range of 6–8 nm existing between the first generation agglomerates still remained in the powder compact, which was prepared under the highest pressure of 300 MPa. Assuming an fcc arrangement of first generation agglomerates, the sizes of the agglomerate are determined to be between 40 and 52 nm, as calculated from the pore radius.[9] Mayo[4] demonstrated that by the dry forming of CIP and uniaxial pressing, unless an ultra high GPa pressure is used, it is impossible to make a homogeneous powder compact from agglomerated nanocrystalline powders.

Fig. 4 shows the effect of isostatic pressure on green density for nanocrystalline ITO powder. The green density of the powder compact increased from 19 to 47% with an increase in the forming pressure. However, the gradient of the density increase was different, i.e. the green density increased steeply to 100 MP and then, it increased slowly above that pressure. Regarding the cumulative pore size distribution, green density increased to 100 MPa of the forming pressure due to the elimination of pores between the inter-second or higher generation agglomerates. A further increase of the green density above 100 MPa was due to shrinkage of the pores between inter-first generation agglomerates. It is noteworthy that the pores were not eliminated yet.

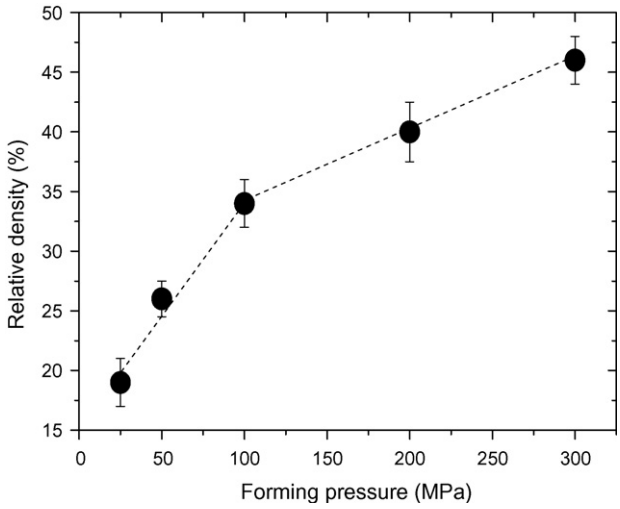

Fig. 4. The effect of the forming pressure on the relative density of the ITO green body.

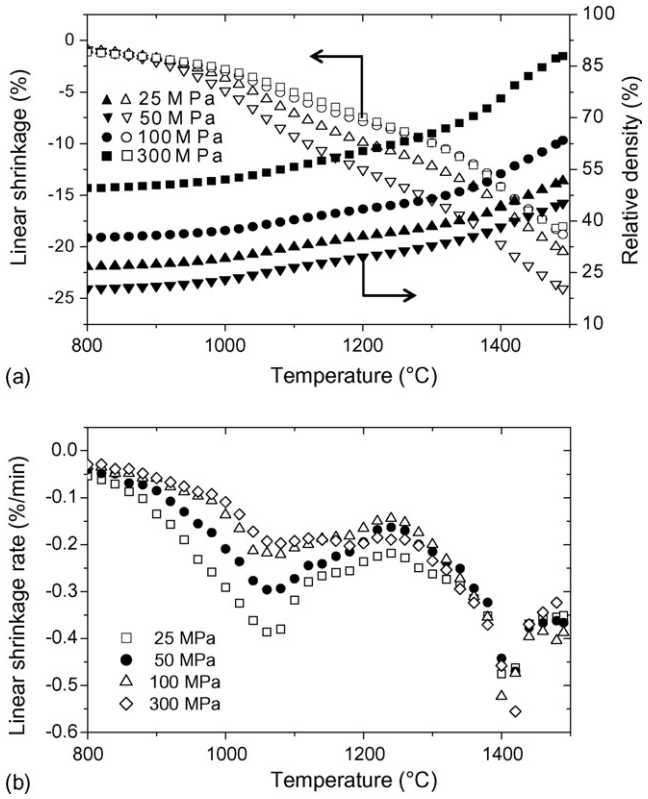

Fig. 5. Linear shrinkage ($\Delta L/L_0$) of the ITO samples during thermo-mechanical analysis in air: (a) linear shrinkage and the relative density calculated from data, (b) derivative of its linear shrinkage with respect to time (the shrinkage rate).

Fig. 5 shows the (a) linear shrinkage and the relative density and (b) the linear shrinkage rate of the ITO samples, with respect to temperature and forming pressure. The density (ρ) of the samples was determined from the green density (ρ_0) and the linear shrinkage $\Delta L/L_0$ by using the following equation: [10]

$$\rho = \frac{\rho_0}{(1 - \Delta L/L_0)^3} \quad (1)$$

where L_0 is the initial length of the sample; L, instantaneous sample length, and $\Delta L = L_0 - L$. The densification of the samples started from 900 °C and increased gradually as the temperature increased. The relative density of the samples at 1500 °C, which is the temperature limit of the TMA equipment used in this experiment, were showed 45, 51, 63, and 87% for the samples prepared under the forming pressure levels of 25, 50, 100, and 300 MPa, respectively. The final density of ITO samples were in proportion to the green density (see Fig. 4).

Significant shrinkage rates appeared at two different temperatures near 1100 and 1400 °C, as shown in Fig. 5(b). This implies that the ITO samples are sintered by two densification steps, operating at low and high temperatures. The great amount of shrinkage, observed at 1100 °C, decreased when the forming pressure increased, but another shrinkage observed at 1400 °C, seemed to be independent of the forming pressure. The two-step densification can be explained by the differential densification[11] due to the inhomogeneities in the powder compact, such as agglomerates, i.e. the first step of densification

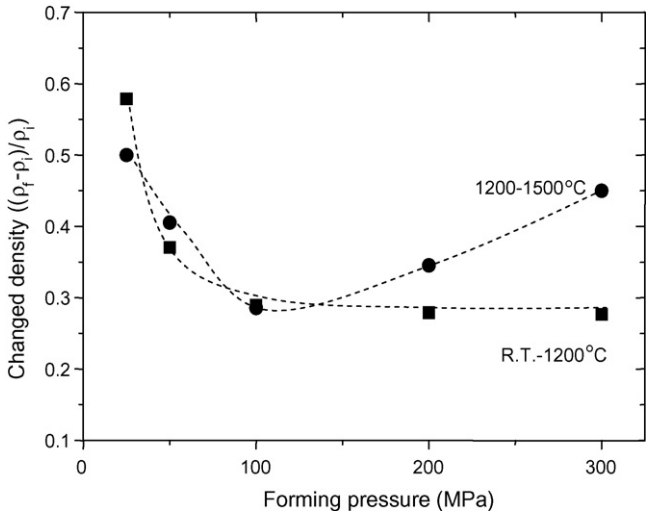

Fig. 6. The changed density of the ITO samples calculated by using the density data of thermo-mechanical analysis as a function of forming pressure.

occurred at a lower temperature through the elimination of small pores between nanocrystalline powders, and the second step of densification progressed at a higher temperatures by eliminating large pores between the agglomerates.

Fig. 6 shows the changes in the density in the two different temperature ranges, room temperature ~1200 °C and 1200–1500 °C, with respect to forming pressure. The changed density was calculated by using the relative density obtained from the TMA experiment as shown in Fig. 5. The changed density, which occurred between room temperature and 1200 °C, decreased to 100 MPa and then, it was almost invariant in samples of >100 MPa. This implies that density changes between room temperature and 1200 °C caused by that densification occurred due to the elimination of the smallest pores between the crystallites which existed in all powder compacts. The changed density decrease in the samples of <100 MPa is attributable to the shrinkage of the large pores and the elimination of the smallest pores between the crystallites. The lack of change in the density for samples >100 MPa implies that the volume of the smallest pores between the crystallites is constant in all powder compacts and that the pores are removed in the first step of densification. The density change between 1200 and 1500 °C decreased to 100 MPa and it increased in samples >100 MPa. The change in density between 1200 and 1500 °C is attributable to densification that occurred by the elimination of pores among the first generation agglomerates.

Fig. 7 shows the fracture surfaces of the ITO samples sintered at 1200 °C without holding time. These samples were prepared under the forming pressure of (a) 25, (b) 50, (c) 100, and (d) 300 MPa, respectively. Agglomerates as large as 10 μm were observed in samples of 25 and 50 MPa. Homogenous microstructures without large agglomerates developed in the ITO samples prepared under >100 MPa because the forming pressure of >100 MPa could break down the second generation agglomerates and further generation agglomerates in the green bodies, as suggested by the pore size distribution curves shown in Fig. 2. Then pores remained in large agglomerates as shown

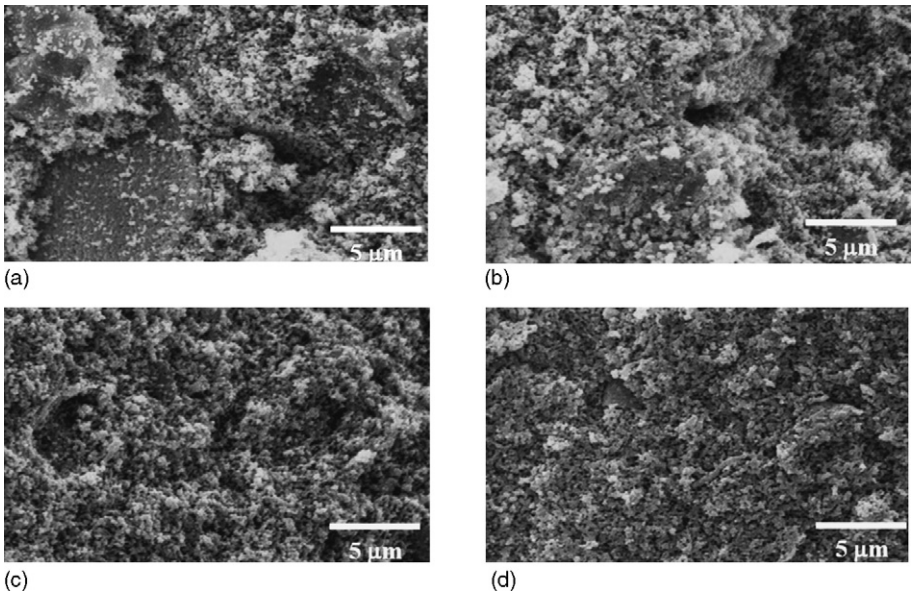

Fig. 7. Fracture surfaces of ITO samples sintered at 1200 °C for 0 h. Forming pressure: (a) 25 MPa, (b) 50 MPa, (c) 100 MPa, and (d) 300 MPa.

in Fig. 7(a) and (b). This implies that the large agglomerates (*n* generation agglomerate) were still not densified at 1200 °C.

Fig. 8 shows the fracture surface of ITO samples after TMA analysis as shown in Fig. 5. These samples were prepared under the forming pressure of (a) 25, (b) 50, (c) 100, and (d) 300 MPa, respectively. Cracks were presented only in samples of 25 and 50 MPa in which large agglomerates were observed at 1200 °C, as shown in Fig. 8(a) and (b). Cracks disappeared and the pore shape morphology changed from cylinder-like to spherical as the forming pressure increased.

Three kinds of powder's void space: void space between crystallites (inter-crystallite pores), void space between first generation agglomerates (inter-first generation agglomerate pores), and void space between second generation agglomerates (inter-second generation agglomerate pores) existed in the powder compacts at low forming pressure. One can visualize these spaces as divided into separate entities or pores, each bounded by a surface of in-contact crystallites. If the in-contact crystallites are not disrupted during heating, the touching particles will first develop bridging necks. Theory backed by empirical observation shows that neck formation in crystalline powders can occur either by evaporation and condensation or by a diffusional process (surface, volume, and/or grain boundary).[12] Once a necks form, further mass rearrangement occurs in an attempt to produce a pore-surface morphology that is determined by the dihedral angle and the pore's coordination number (which here-

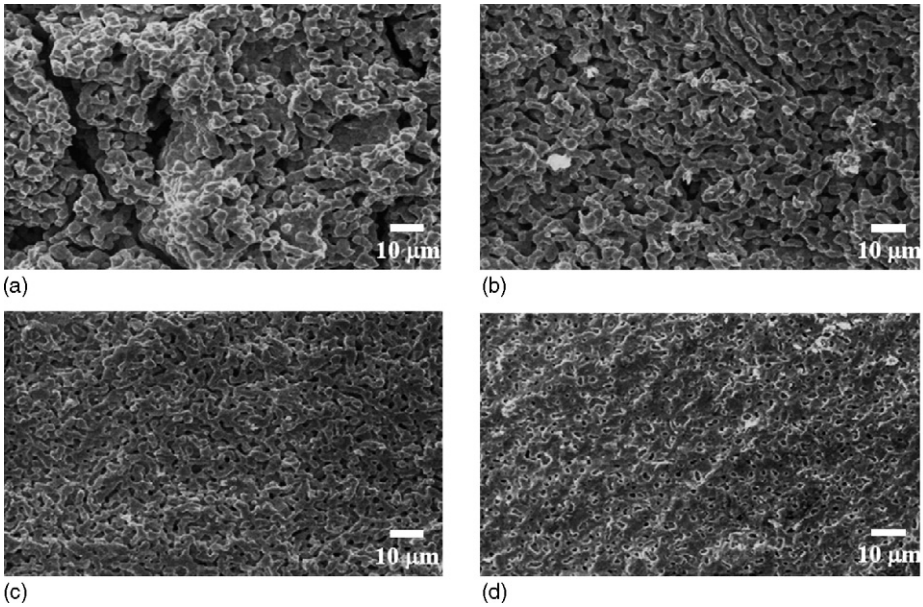

Fig. 8. Fracture surfaces of the ITO samples sintered at 1500 °C for 0 h. The sintering of the samples was carried out with TMA equipment. Forming pressure: (a) 25 MPa, (b) 50 MPa, (c) 100 MPa, and (d) 300 MPa.

after is denoted as R). Since the dihedral angle is constant in the same system, R determines the pore-surface morphology of ITO.

Lange[13] suggested that the higher R has convex surfaces, whereas a lower R has concave surfaces. In addition, he suggested that for a given dihedral angle, a critical coordination number, R_C, exists that defines the transition from convex to concave surfaces. Kingery and Francois[14] were the first to recognize that only those pores with $R < R_C$ are able to disappear during sintering. To eliminate the pores with $R > R_C$, they must decrease their R through gain growth. Pores with $R > R_C$ can be removed more readily at higher temperature than pores that have $R < R_C$ in the case of the same sintering time.

As previously noted, at low sintering temperatures, a nanocrystalline ITO compact is sintered by the elimination of inter-crystallite pores, which are small and have a low R. Actually, the inter-crystallite pore radius of the nanocrystalline ITO powder compact used in this experiment is between 3 and 6 nm as calculated by the crystallite size. At high sintering temperatures, the compact is sintered by the elimination of inter-first generation agglomerate pores, which are large and have a high R. This sintering behavior leads to a two-step densification in the TMA experiments with a nanocrystalline ITO compact. Then crack-like voids are observed in samples that are formed under low pressure and sintered at 1500 °C. To eliminate crack-like voids which are thermodynamically stable, samples were sintered at higher temperatures. However, since an ITO system has high evaporation at $T > 1200$ °C, increasing the sintering temperature so as to eliminate crack-like voids is ineffective in ITO samples.

4. Conclusions

The homogeneity of the powder compacts fabricated with agglomerated nanocrystalline ITO powders was investigated as a function of cold isostatic pressing pressure. In addition, the sintering behavior of the powder compacts was investigated using a TMA experiment and is discussed with respect to the elimination of pores. An increase in the forming pressure enhances the homogeneity of the powder compact by crushing large agglomerates. The first generation agglomerate in a green body, however, cannot be destroyed by the highest forming pressure of 300 MPa because nanocrystalline powder has a large number of particle–particle point contacts per unit volume, as compared with powder that has micrometer-sized particles. The first generation agglomerate compact shows a two-step densification in the shrinkage rate curve of the TMA which can be explained by the elimination of two kinds of pores: small inter-crystallite pores and large inter-first generation agglomerate pores.

Acknowledgments

This work was supported by the National Research Laboratory grant from the Ministry of Science and Technology (MOST) and the Korea Science and Engineering Foundation (KOSEF).

References

1. Stokes, R. J. and Evans, D., *Fundamentals of Interfacial Engineering*. Wiley-VCH, Inc, New York, 1996, pp. 24–33.
2. Mayo, M. J., Processing of nanocrystalline ceramics from ultrafine particle. *Int. Mater. Rev.*, 1996, **41**, 85–115.
3. Onoda, G. Y. and Toner, J., Fractal dimensions of model particle packings having multiple generations of agglomerates. *J. Am. Ceram. Soc.*, 1986, **69**, C-278–C-279.
4. Mayo, M. J., Processing of nanocrystalline ceramics from ultrafine particles. *Int. Mater. Rev.*, 1996, **41**, 85–115.
5. Kim, B. C., Kim, S. M., Lee, J. H. and Kim, J. J., Effect of phase transformation on the densification of coprecipitated nanocrystalline ITO powders. *J. Am. Ceram. Soc.*, 2002, **85**, 2083–2088.
6. Nadaud, N., Nanot, M. and Boch, P., Sintering and electrical properties of titania- and zirconia-containing In_2O_3–SnO_2 (ITO) ceramics. *J. Am. Ceram. Soc.*, 1994, **77**, 843–846.
7. De Wit, J. H. W., Laheij, M. and Elbers, P. F., Grain growth and sintering of In_2O_3. *Sci. Ceram.*, 1997, **9**, 143–150.
8. JCPDS card for cubic indium tin oxide #06-0416.
9. James, S., *Reed Principles of Ceramics Processing*. John Wiley & Sons, New York, 1995, pp. 221–221.
10. Rahaman, M. N., *Ceramic Processing and Sintering*. Marcel Dekker, Inc, New York, 1995, pp. 683–685.
11. Halloran, J. W., Role of powder agglomerates in ceramic processing. In *Forming of Ceramics, Advances in Ceramics*, *Vol. 9*, ed. J. A. Mangles. American Ceramic Society Inc, Columbus, Ohio, 1984, pp. 67–75.
12. Coble, R. L., Development of microstructure in ceramic systems. In *Ceramic Microstructures*, ed. R. M. Fulrath and J. A. Pask. John Wiley & Sons, Inc, New York, 1968, pp. 658–680.
13. Lange, F. F., Sinterability of agglomerated powders. *J. Am. Ceram. Soc.*, 1984, **67**, 83–89.
14. Kingery, W. D. and Francois, B., Sintering of crystalline oxides interactions between grain boundaries and pores. In *Sintering and Related Phenomena*, ed. G. C. Kuzynski, N. A. Hooton and G. F. Gibbon. Gordon Breach, New York, 1967, pp. 471–498.